

3-D electromagnetic imaging of a Palaeozoic plate-tectonic boundary segment in SW Iberian Variscides (S Alentejo, Portugal)

N. Vieira da Silva^a, A. Mateus^b, F.A. Monteiro Santos^{a,*}, E.P. Almeida^{a,c}, J. Pous^d

^a *Uni. de Lisboa, CGUL-IDL, Ed. C8, Piso 6, Campo Grande, 1749-016 Lisboa, Portugal*

^b *Uni. de Lisboa, Dep. Geologia and CREMINER, Ed. C6, Piso 4, Campo Grande, 1749-016 Lisboa, Portugal*

^c *Instituto Politécnico de Tomar, 2300 Tomar, Portugal*

^d *Dep Geodinàmica i Geofísica, Uni. Barcelona, Martí Franques s/n, 08028 Barcelona, Spain*

Received 1 December 2005; accepted 25 June 2007

Available online 28 July 2007

Abstract

In SW Iberian Variscides, the boundary between the South Portuguese Zone (SPZ) and the Ossa Morena Zone (OMZ) corresponds to a major tectonic suture that includes the Beja Acebuches Ophiolite Complex (BAOC) and the Pulo do Lobo Antiform Terrane (PLAT). Three sub-parallel and approximately equidistant MT profiles were performed, covering a critical area of this Palaeozoic plate-tectonic boundary in Portugal; the profiles, running roughly along a NE–SW direction, are sub-perpendicular to the main Variscan tectonic features. Results of the three-dimensional (3-D) modelling of MT data allow to generate, for the first time, a 3-D electromagnetic imaging of the OMZ–SPZ boundary, which reveals different conductive and resistive domains that display morphological variations in depth and are intersected by two major sub-vertical corridors; these corridors coincide roughly with the NE–SW, Messejana strike–slip fault zone and with the WNW–ESE, Ferreira–Ficalho thrust fault zone. The distribution of the shallow resistive domains is consistent with the lithological and structural features observed and mapped, integrating the expected electrical features produced by igneous intrusions and metamorphic sequences of variable nature and age. The development in depth of these resistive domains suggests that: (1) a significant vertical displacement along an early tectonic structure, subsequently re-taken by the Messejana fault-zone in Late-Variscan times, has to be considered to explain differences in deepness of the base of the Precambrian–Cambrian metamorphic pile; (2) hidden, syn- to late-collision igneous bodies intrude the meta-sedimentary sequences of PLAT; (3) the roots of BAOB are inferred from 12 km depth onwards, forming a moderate resistive band located between two middle-crust conductive layers extended to the north (in OMZ) and to the south (in SPZ). These conductive layers overlap the Iberian Reflective Body (evidenced by the available seismic reflection data) and are interpreted as part of an important middle-crust *décollement* developed immediately above or coinciding with the top of a graphite-bearing granulitic basement.

© 2007 Elsevier B.V. All rights reserved.

Keywords: Electromagnetic imaging; 3-D modelling; Magnetotellurics; SW Iberian Variscides

1. Introduction

The SW Iberian Variscides represents one of the key segments of the European Variscan Fold Belt (Lötze, 1945;

Julivert et al., 1980; Ribeiro, 1981; Quesada, 1991), whose structure resulted from the oblique continental collision operated in Carboniferous involving three main geotectonic units, from north to south: the Central-Iberian Zone (CIZ), the Ossa Morena Zone (OMZ) and the South Portuguese Zone (SPZ). The boundaries of these units correspond, therefore, to major suture zones, regardless of

* Corresponding author.

E-mail address: nmysilva@fc.ul.pt (N. Vieira da Silva).

diverse controversial issues concerning particular lithological and structural data that record the early stages of their geodynamic evolution (Bard et al., 1973; Matte, 1986; Munhá et al., 1989; Ribeiro et al., 1990; Ábalos and Díaz Cusí, 1995; Simancas et al., 2001; San José et al., 2004).

In the past two decades, many studies were devoted to the OMZ–SPZ boundary in order to decipher its constitution and internal architecture, thus contributing to a better understanding of this suture zone. Critical advances were made after comprehensive geological mapping and structural analysis, coupled by detailed investigations on stratigraphy, geochemistry and (metamorphic and igneous) petrology (see references in Section 2). Concurrently, important progresses were recorded on geochronology (see references in Section 2), bringing light to several critical questions and limiting hypotheses postulated in some geodynamic models. Data obtained from these multidisciplinary research programmes were recently complemented by magnetotelluric (MT) surveys intended

to elucidate the structural arrangement at depth (Monteiro Santos et al., 1999; Almeida et al., 2001; Monteiro Santos et al., 2002; Pous et al., 2004; Almeida et al., 2005). Additionally, a deep seismic reflection profile was performed, but crossing only the Spanish counterpart of the OMZ–SPZ boundary (Simancas et al., 2003, 2004; Carbonell et al., 2004). Despite all the available data, many issues are still open to debate, clearly demonstrating the inherent complexity of this plate-tectonic boundary. This justifies added efforts in order to provide supplementary elements that enable to improve the existing knowledge on the SW Iberian Variscides.

One of the issues that need further investigation concerns the lateral continuity of deep structures in the OMZ–SPZ boundary, therefore helping to precise the suture geometry and the extension/morphology of major *décollements* expected to exist at middle to lower crustal depths in both sides of the suture. This can be done by different means, although MT survey has already proved

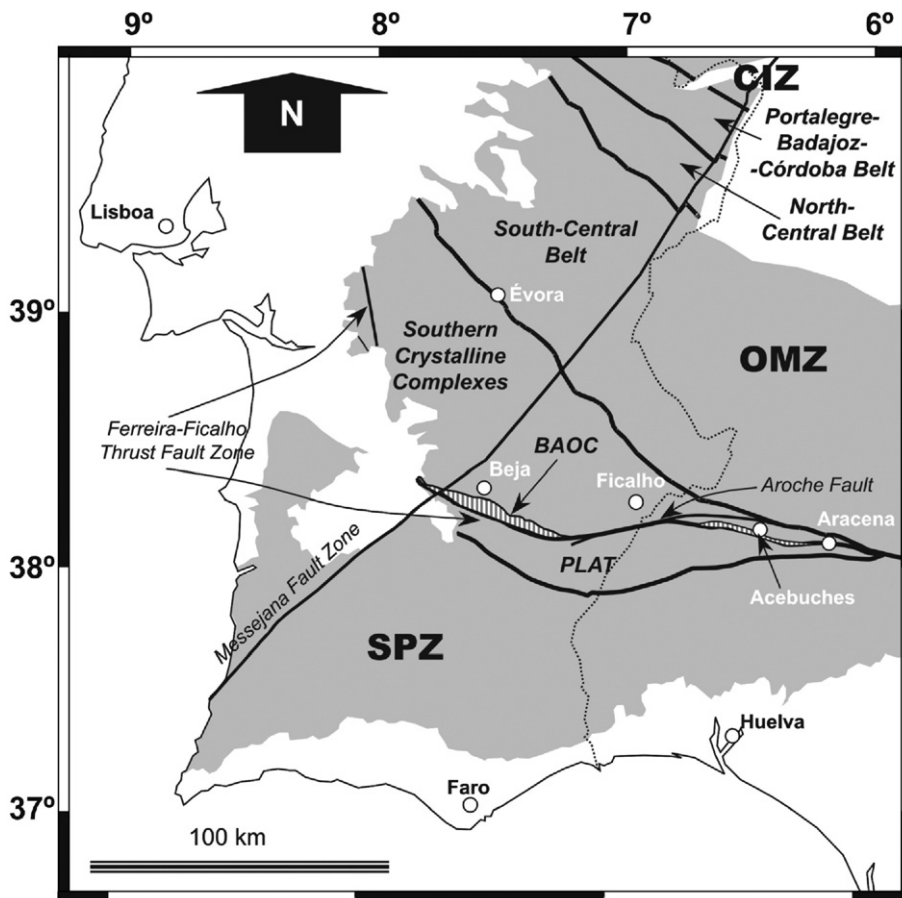


Fig. 1. A — The main geotectonic units of SW Iberian Variscides and schematic representation of the OMZ belts. B — Simplified geological map of the OMZ southern border, Exotic Terranes and SPZ northern border (adapted from the Geological Map of Portugal, 1:500,000 scale, 1992 — J.T. Oliveira and E. Pereira, compilers). The aligned dots represent the sites of the three MT profiles performed.

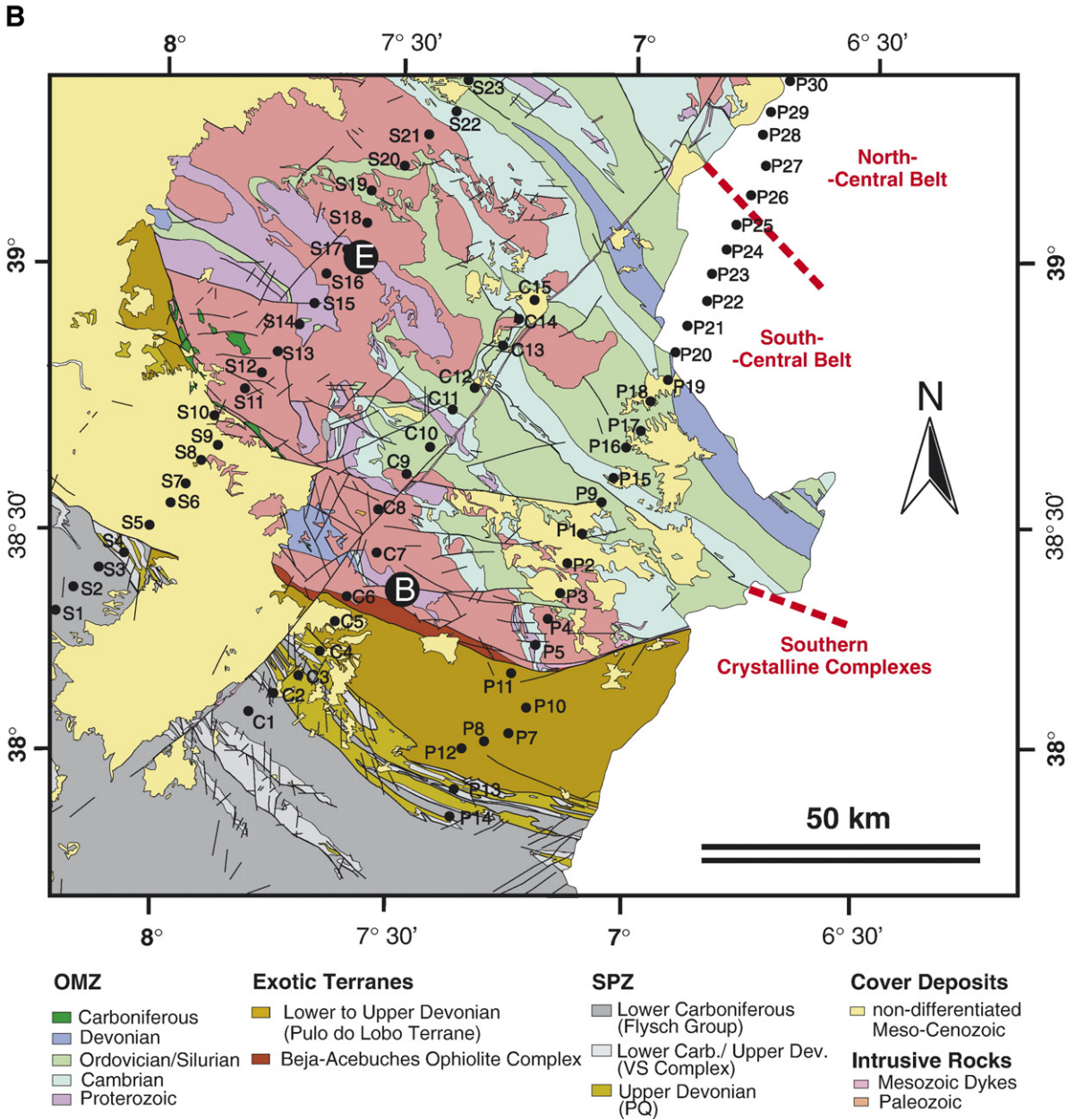


Fig. 1 (continued).

to be an adequate tool for unravelling a significant part of that pattern, mostly because of the presence of high conductivity contrasts and of the profusion of late vertical structures. In the Spanish counterpart of the OMZ–SPZ boundary, the confronting of MT with seismic reflection data (Simancas et al., 2003; Carbonell et al., 2004; Pous et al., 2004) provided important evidences for the interpretation of deep structures and opened to debate a new problem: the meaning of a 2 s thick reflective and conductive band, known as Iberian Reflective Body

(IRB). In the Portuguese sector of the boundary, a third MT profile was recently carried out, thus complementing results previously gathered in two other sub-parallel profiles (Almeida et al., 2001; Monteiro Santos et al., 2002; Almeida et al., 2005). Therefore, data from these MT profiles can be used to produce, for the first time, a 3-D electromagnetic imaging of this plate-tectonic boundary, allowing also discussing the earlier interpretations proposed for IRB. This two-fold objective is, consequently, the aim of the present work.

2. Geological setting

The three sub-parallel and approximately equidistant MT profiles, roughly running NE–SW, cross a critical region of the SW Iberia Variscides (Fig. 1A). This region includes both the borders of OMZ, to the north, and SPZ, to the south, besides the exotic terranes positioned between them: the Beja Acebuches Ophiolite Complex (BAOC) and the Pulo do Lobo Antiform Terrane (PLAT). A general outline of the geological background presented by this region will be made according to the multidisciplinary data available for each unit and terrane, from north to south. In this overall assessment, particular emphasis will be given to the lithological and structural characteristics considered relevant for the interpretation of MT data.

On the basis of palaeogeographic, igneous, metamorphic and structural features it is usual to organise the OMZ into different belts, the most widely accepted division being that reported in *Apalategui et al. (1990)*. The region of concern encompasses the two southernmost OMZ belts separated by a major thrust zone, *i.e.* the SE part of the South-Central Belt and the Southern Crystalline Complexes (Fig. 1B).

The SE part of the South-Central Belt is largely dominated by different sedimentary and volcanic sequences from Cambrian to Devonian ages (*Oliveira et al., 1991*) that are locally intruded by Late-Variscan granitoids (the Reguengos de Monsaraz granodiorite being the most outstanding igneous body) and covered by Cainozoic clastic sediments. In short, the Lower Cambrian sequences are dominated by meta-dolostones with several intercalations of meta-volcanic rocks and topped by a discontinuous silico-ferruginous horizon. The Upper Cambrian–Ordovician sequences are made of marbles and (bimodal) meta-volcanics, sometimes containing intercalated meta-pelitic/psammitic levels. The Ordovician sequences are essentially composed of metapelites and psammites, whose base includes different horizons of bimodal meta-volcanics, evolving to quartzites towards the top. The Silurian–Lower Devonian sequences are mostly composed of slaty and meta-psammites. The Upper Devonian comprises a flysch-type series where greywackes prevail. All these rocks show strong recrystallisation and deformation developed during the Variscan Orogeny; metamorphism grades from greenschist to transitional greenschist–amphibolite facies conditions (*Quesada and Munhá, 1990*); deformation is multiphase and its effects observed at all scales (*Araújo, 1995; Fonseca, 1995*). Late strike–slip fault zones, developed in the waning stages of the Carboniferous continental collision, intersect all the previous structures. One of the most remarkable elements of the Late-Variscan

fracture network (*Arthaud and Matte, 1975; Marques et al., 2002*) is the Messejana strike–slip fault, which can be followed for approximately 530 km. This fault zone was successively re-activated during the Alpine Orogeny, as documented both by multiple injections of dolerite rocks (*Martins, 1991; Cebriá et al., 2003*) and distinct displacements caused in geological formations of different ages.

The Southern Crystalline belt internal architecture is more complex than the one showed by the SE part of the South-Central Belt. This complexity is due to different causes, but mostly to the following (*Jesus et al., 2007*): 1) high abundance of igneous intrusions that form different petrogenetic suites generated and emplaced under distinct conditions from Early to Late-Variscan times; 2) widespread development of Early Variscan thrust zones, leading to significant tectonic stacking and strain partitioning; and 3) extensive formation of Variscan, sub-vertical shear zones, often contributing to considerable horizontal displacement and strong dismembering of the pre-existent geological framework.

Although still open to controversial issues, the correlations so far carried out in different sectors of the Southern Crystalline Complexes (*Oliveira et al., 1991; Araújo, 1995; Rosas, 2003*), allow the re-construction of a general litho-stratigraphic column. The older sequences (Upper Proterozoic) are well represented in the NW part of the belt and comprise a tectonically imbricate series of black schists and meta-cherts, mica-schists, amphibolites and strongly re-crystallised felsic meta-volcanics; locally, levels of black quartzites, slates and meta-greywackes can also be identified. The Cambrian to Ordovician sequences are lithologically similar to those in the SE part of the South-Central Belt, although showing a more complex internal framework because of multiphase thrusting. In sequences dated of Silurian, slates and psammites prevail over lites and meta-volcanic rocks, forming a relatively monotonous, rather deformed and thick series interpreted by some authors (*Araújo et al., 2005*) as tectonic *mélanges*. The uppermost sequences (Devonian to Carboniferous) are present in small windows preserved among some components of the igneous complexes outcropping in the NW part of the belt; they comprise mostly meta-limestones, different types of clastic meta-sediments, abundant meta-volcanic rocks of variable chemical nature and scarce coal beds. Two Variscan metamorphic events can be put in evidence in the Southern Crystalline belt: the older one is recorded by eclogite/blueschist rocks preserved in early nappe systems (*Fonseca et al., 1999; Moita et al., 2005a*); the later one, developed during the oblique continental collision, has a regional character and grades from greenschist to transitional greenschist–amphibolite facies conditions (*Quesada and Munhá, 1990*). Effects of

the multiphase Variscan deformation are strong and observed at all scales (Silva et al., 1990b; Araújo, 1995; Araújo and Ribeiro, 1995; Fonseca, 1995; Rosas, 2003).

As referred above, late- to post-collision igneous bodies are profuse in the Southern Crystalline Complexes, locally developing evident aureoles of contact metamorphism (Andrade, 1983; Santos et al., 1990; Dallmeyer et al., 1993; Pin et al., 1999; Gomes, 2000; Jesus et al., 2003; Moita et al., 2005b,c). From NW to SE it is worth to note: (1) the large Évora Massif, mostly composed of granitoid rocks that in the Montemor-o-Novo region are clearly related to anatexis processes; (2) the huge and multiphase igneous complex of Beja, comprising a wide range of gabbroic, diorite and granitoid porphyry rocks; and (3) the relatively extensive late granite body of Pias-Pedrogão. Together, these three major igneous masses form an almost continuous, wide curved band that is put in contact with the southern exotic terranes through re-activated Variscan shear zones or Late-Variscan strike-slip fault zones.

The BAOC forms a tectonically dismembered ophiolite sequence incorporated in the South Iberia Variscan Suture (Munhá et al., 1986, 1989; Quesada, 1991; Fonseca and Ribeiro, 1993; Quesada et al., 1994; Figueiras et al., 2002; Díaz Aspiroz et al., 2004). The lower and intermediate sections of BAOC comprise meta-peridotites and meta-gabbroic rocks, respectively, and preserve early anisotropic fabrics indicating northwards shearing, being affected by late multistage metasomatism in domains adjoining the Variscan shear zones. The upper sections of BAOC consist essentially of amphibolites derived from basaltic lavas of tholeiitic nature. Both the northern and southern limits of BAOC are tectonic, actually corresponding to (re-activated) reverse-sinistral WNW–ESE shear zones with strong dip towards SSW (Mateus et al., 1999; Figueiras et al., 2002).

The Ferreira–Ficalho thrust zone marks the present contact between PLAT and OMZ or BAOC and PLAT, being displaced by the ENE–WSW, sub-vertical Aroche–Ficalho strike-slip fault. From the available data (Mateus et al., 1999; Figueiras et al., 2002), the Ferreira–Ficalho thrust zone does not represent the original BAOC–PLAT contact, but simply a shallow expression of a re-activated deep and more complex structure developed in the course of the OMZ–SPZ late-collision stages.

The PLAT is composed of distinct meta-sedimentary successions that locally include bimodal meta-volcanic rocks (with prevalence of the mafic, tholeiitic terms) and display strong multiphase Variscan deformation. These successions can be grouped in three main stratigraphic Formations that, according to the available palynological data, range from Lower–Middle Devonian to Givetian–

Frasnian (Carvalho et al., 1976; Oliveira et al., 1986; Giese et al., 1988; Oliveira, 1990). Metamorphic conditions are of lower greenschist facies, although rocks belonging to the uppermost Formation may reveal anchimetamorphic features (Munhá, 1990). Even pointing out several dissimilarities in geometry or in structural interpretation, the works performed in several sectors of PLAT enable to recognise different phases of folding/axial plane cleavage development, besides important thrust systems with prevailing southwards shear sense (Silva et al., 1990a,b; Onézime et al., 2002). In this context, it should be emphasised the presence of the late- to post-collision granodiorite of Gil Marquez in the Spanish counterpart of PLAT, regardless of the absence of similar igneous bodies outcropping in Portugal.

The SPZ northern border corresponds approximately to the Iberian Pyrite Belt (IPB), which comprises a succession of three Palaeozoic stratigraphic Formations affected by low-grade metamorphism. The older meta-sedimentary sequence, whose footwall remains cryptic, is the Phyllite–Quartzite Formation dated of Fammenian (Van den Boorgard, 1963; Pereira et al., 1996). Lying upon, the Volcano–sedimentary Complex is composed of a bimodal volcanic suite (despite of the large predominance of felsic units, hosting world-class VMS deposits) inter-fingered with diverse meta-sedimentary rocks (Schermerhorn, 1971; Strauss et al., 1981; Munhá, 1983a,b; Carvalho et al., 1999; Relvas, 2000; Abad et al., 2001). The VS Complex is diachronic, ranging from Early Fammenian to Late Visean (Oliveira, 1983; Marcoux et al., 1992; Nesbitt et al., 1999; Barrie et al., 2002; Oliveira et al., 2004). The later stratigraphic sequence in IPB consists of the Flysch Group, Lower Carboniferous in age (Schermerhorn, 1971; Oliveira, 1983). The major structural feature of IPB corresponds to a south verging thrust–fold belt that defines a thin-skinned structural arrangement developed on top of a major cryptic *décollement* believed to coincide with the lower–upper Devonian transition within PQ Formation (Prodehl et al., 1975; Ribeiro and Silva, 1983; Silva et al., 1990a,b; Quesada, 1998; Onézime et al., 2002; Soriano and Casas, 2002).

3. Magnetotelluric data

The MT method allows the investigation of the electrical conductivity distribution downward the earth from simultaneous measurements of natural variations of the surface electric (E) and magnetic fields (H) over a broad band of frequencies (see, e. g., Vozoff, 1991). For plane wave source fields, the horizontal components of electric and magnetic fields are connected via the linear

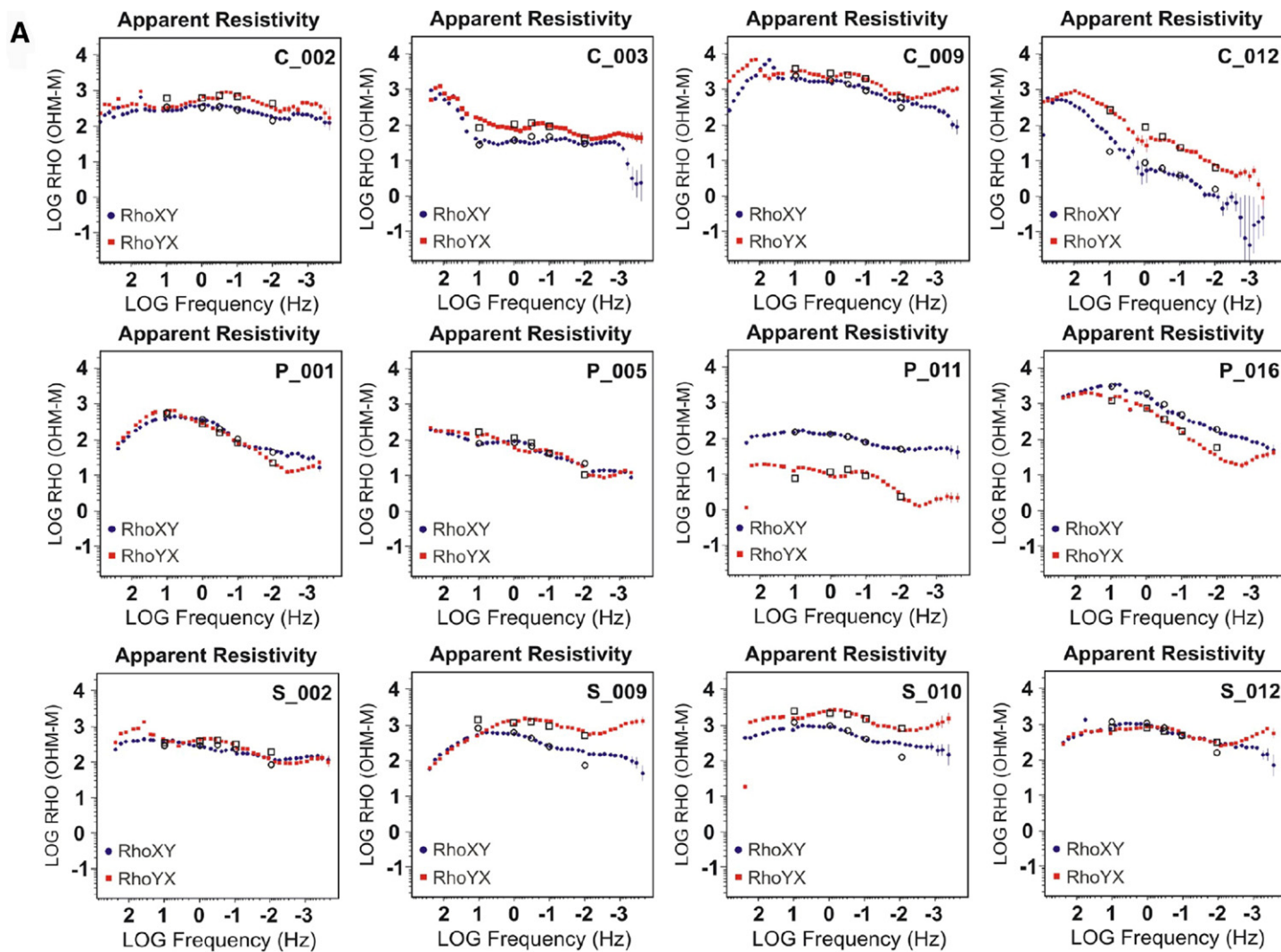


Fig. 2. Data (solid symbols) and model responses (open symbols). (A) Apparent resistivities. (B) Phases.

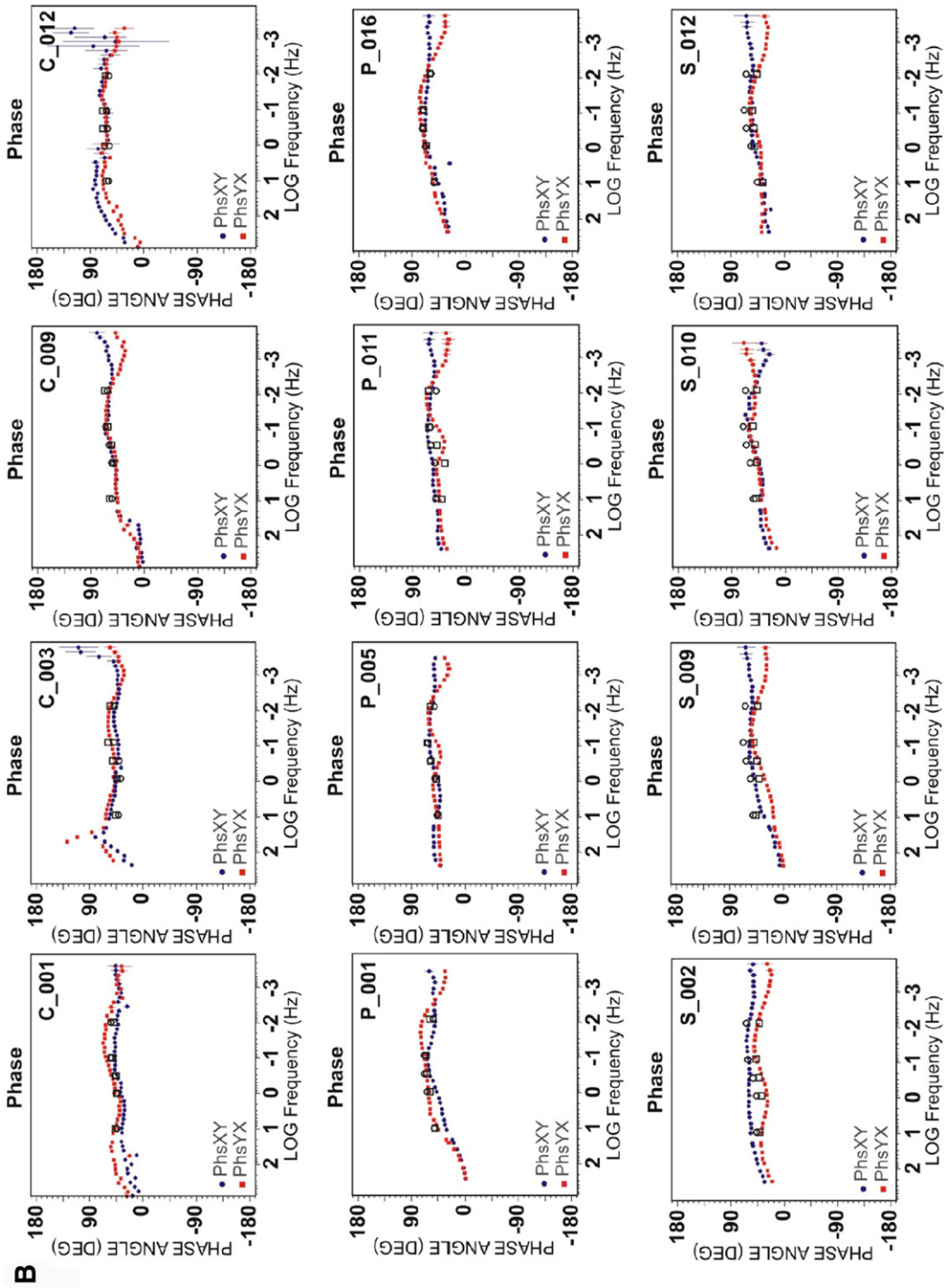


Fig. 2 (continued).

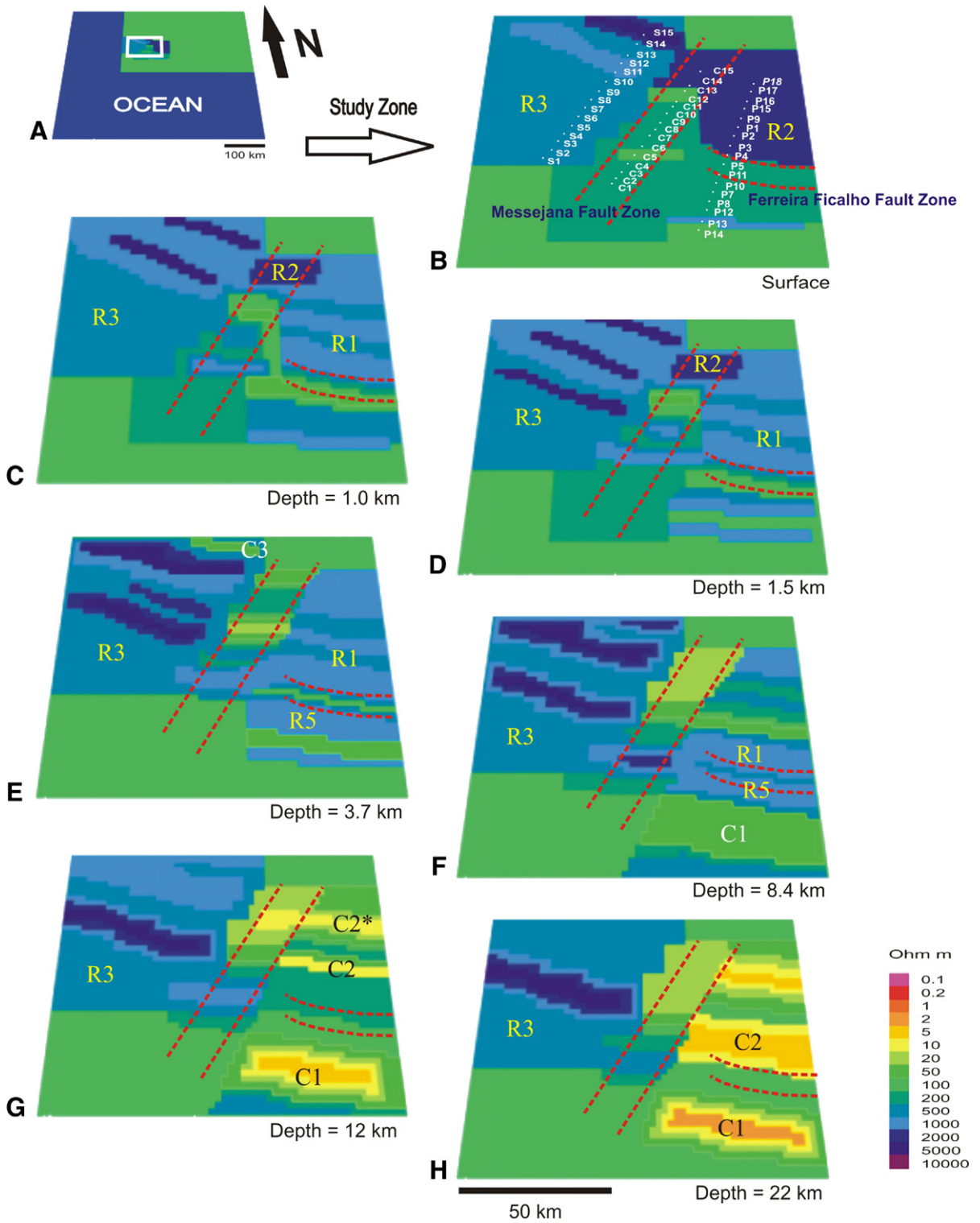


Fig. 3. Horizontal slices of the 3-D resistivity model. (A) General view of the 3-D model core with the Atlantic Ocean effect included. (B) Uppermost slice of the 3-D model in the study area. (C) Slice of the 3-D model in the study area at 1.0 km. (D) Slice of the 3-D model in the study area at 1.5 km. (E) Slice of the 3-D model in the study area at 3.7 km. (F) Slice of the 3-D model in the study area at 8.4 km. (G) Slice of the 3-D model in the study area at 12 km. (H) Slice of the 3-D model in the study area at 22 km. Vertical cross-sections of the 3-D model approximately coincident with the MT profiles P, C and S.

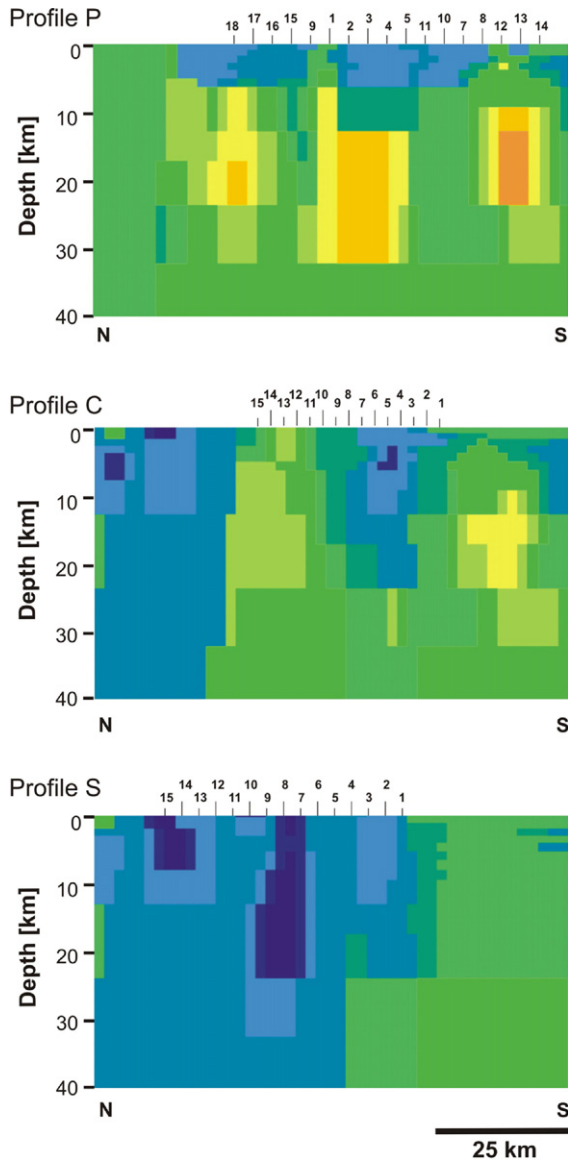


Fig. 3 (continued).

relationship: $E = ZH$. The anti-diagonal elements of the impedance tensor (Z), that describe the resistivity structure beneath the measuring site, are used to calculate the apparent resistivity functions, ρ_{xy} and ρ_{yx} and the phase functions, ϕ_{xy} and ϕ_{yx} , that are defined as:

$$\begin{aligned}\rho_{xy} &= |Z_{xy}|^2 / (\omega\mu_0) \\ \rho_{yx} &= |Z_{yx}|^2 / (\omega\mu_0) \\ \phi_{xy} &= \arg(Z_{xy}) \\ \phi_{yx} &= \arg(Z_{yx})\end{aligned}$$

where ω represents the angular frequency and μ_0 is the magnetic permeability of the vacuum.

Fig. 2 shows the apparent resistivities and phases for 12 sites (four sites from each of the profiles). The apparent resistivity and phase curves are shown in the measurement referential (N–S and E–W). The apparent resistivity curves of sites on profile C shows an increase in the slope as the structures are crossed from south to north. These types of trends are also observed in MT data from profile P but not in the data from sites located in the profile S. This suggests that the resistivity distribution in the western part of the survey is different from that one in the eastern part. The changes in the resistivity distribution seem to be controlled by the Messejana fault.

The Groom-Bailey tensor decomposition was applied to the measured data set associated with each profile, resolving the single-site regional strike angles. After that, the multi-site, multi-period analysis was applied to the data in order to check a common strike direction for each profile. This method calculates a common strike for all the sites in a determined frequency range by minimising the global χ^2 misfit. The determination of such strike is a fundamental step for 2-D model inversion. Prior to the inversion procedure, the static shift galvanic distortion must be considered. This distortion shifts the rotated logarithmic apparent resistivity curves by a frequency-independent factor while the phase curves remain unchanged. The scattering in levels of the apparent resistivity curves within each zone was less than one decade and the levels of the curves were shifted accordingly. During the inversion procedure some static shifts were corrected at those sites with a poor fit.

4. 3-D modelling

For 3-D modelling, the 2-D models obtained from the inversion of each profile complemented with the geological information available for that area were considered. The 2-D inversion of rotated apparent resistivity and phases for both modes was carried out using the REBOCC code (Siripunvaraporn and Egbert, 2000). For the inversion procedure, the Atlantic Ocean, at southward, was included as a fixed parameter and an approximate bathymetry representation and resistivity value of $0.3 \Omega \text{ m}$ were accounted. To achieve a good fit in 2-D models, the inversion was carried out using an iterative scheme. First, the rotated geomagnetic transfer functions (real and imaginary) were inverted from a homogeneous half-space. Second, the final model was used as an initial one for the inversion of TM data and rotated geomagnetic transfer functions. Finally, the resulting model was used as an initial one for the joint inversion of TE and TM and rotated geomagnetic transference functions. The final resistivity models have RMS misfits between 2.9 and 4.9.

The three-dimensional modelling was performed using the Mackie 3-D forward code (Mackie et al., 1994). A mesh of $71 \times 70 \times 34$ cells, in the N–S, E–W and vertical directions, respectively, was used in the calculations. It should be noted that even with such a mesh the complex geology of the area is only roughly represented. Considering that adjacent MT sites are spaced 5–10 km, some small-scale superficial structures were omitted in modelling. The Atlantic Ocean was also included in the 3-D model, considering a rough bathymetry representation. The conductivity model considered for the lithosphere beneath the ocean was the one presented in Monteiro Santos et al. (2003). Model responses were calculated for 5 periods covering the data range (0.1, 1, 3.12, 10 and 100 s) and for 47 soundings around Messejana and Ferreira–Ficalho fault zones. This period range ensures that numerical instabilities will not occur. In fact, it is sufficient that $|k|z \leq 0.3$ (Mackie et al., 1994) with $|k| = 2/\delta$, where k is the wave number, δ is the skin depth and z is the thickness of the first layer. The upper layers of our grid are discretized at 100 m intervals. If we consider a surface resistivity of $100 \Omega \text{ m}$, then the minimum critical period is 0.02 s. This ensures that the 3-D model period range will not cause numerical instability. The 2-D boundary conditions of the 3-D model were imposed at a distance of 280 km from the old suture and the 1-D boundary condition was imposed at the bottom of the earth model at a depth of 300 km. Fig. 3 shows the final 3-D model obtained by trial and error and Fig. 2 shows the apparent resistivity and phase curves (3-D model response and field data). The xx and yy components of the impedance tensor were not considered on the trial and error procedure to fit the model parameters, because of the high noise level on them.

Seven parallel slices of the final 3-D model for the surveyed region are reported in Fig. 3, forming an ordered sequence that increases in depth. The obtained electromagnetic imaging put in evidence different conductive (C) and resistive (R) domains that display morphological variations at depth and are intersected by two major sub-vertical corridors roughly oriented NE–SW and WNW–ESE. These corridors coincide with the location of the Messejana strike–slip fault zone and the Ferreira–Ficalho thrust fault zone, respectively.

The area covering the geological formations belonging to OMZ (sites 12 to 15 in Profile S, sites 7 to 15 in Profile C and sites 5 to 18 in Profile P) exhibits an overall resistivity higher than $500 \Omega \text{ m}$ in the first 8.4 km depth, despite the split created by the sub-vertical NE–SW corridor after 3.7 km depth. At greater depths ($\geq 8.4 \text{ km}$), this corridor separates a relatively high-resistive sector ($500\text{--}1000 \Omega \text{ m}$), towards NW, from a moderate- to low-

resistive sector ($<200 \Omega \text{ m}$), towards SE, that include a W–E conductor ($<20 \Omega \text{ m}$) well defined from 12 to 22 km depth. However, a careful observation of slices in Fig. 3 allows differentiating several features that are believed to characterise the internal architecture of both the shallowest resistive block and the two deepest major sectors. Indeed, the R1 domain ($500\text{--}1000 \Omega \text{ m}$) appears to be confined to depths ranging from 1.0 to 8.4 km, its NW limit being controlled by the NE–SW sub-vertical corridor. In the first 0.5 km of depth, the large R2 domain ($1000\text{--}2000 \Omega \text{ m}$) overlaps the R1 signal. Between 1.0 and 1.5 km depths R2 is limited to narrow area, completely disappearing in subsequent deeper slices. In shallower sections, the NW edge of R2 is apparently connected to a high-resistive ($2000\text{--}5000 \Omega \text{ m}$) WNW–ESE band that roughly preserves its location and direction till 1.5 km depth, slightly rotating towards W and moving to SSW for greater depths. This S–SW dipping element is no longer observed after 12 km depth; it seems, therefore, that the WNW–ESE band does not have the same geological meaning of R2. For depths above 8.4 km, the prevalent resistive structure is replaced by a conductive one, being worth noting the R1 rupture already caused by a higher conductive zone ($50\text{--}100 \Omega \text{ m}$) at that depth. Two sub-parallel conductive ($5\text{--}10 \Omega \text{ m}$) bands (C2 and C2*) emerge at 12 km depth, separated by a slightly resistive ($50\text{--}100 \Omega \text{ m}$) and somewhat diffuse narrow area. The southern band seems to be more important, extending and enlarging towards deeper levels; at 22 km depth, its S-limit coincides with the WNW–ESE sub-vertical corridor. The W extension of C2* at 12 km depth appears to reinforce the conductive feature related to the NE–SW sub-vertical corridor. According to the results obtained, it is plausible to admit that C2 and C2* correspond to a sole conductor, roughly occupying the area beneath R1 and going deeper, at least till 22 km.

The area covering the geological formations belonging to SPZ–PLAT–BAOC (sites 1 to 11 in Profile S, sites 1 to 6 in Profile C and sites 11 to 14 in Profile P) shows two distinct domains separated by the NE–SW sub-vertical corridor. The first one occupies the entire NW sector and is characterised by an extensive resistive domain (R3, usually $500\text{--}1000 \Omega \text{ m}$) that can be followed till the depth of 22 km. The R3 domain reveals an internal WNW–ESE high-resistive band ($2000\text{--}5000 \Omega \text{ m}$) that, in deeper slices, is drifted towards SW, possibly experiencing an oblique tectonic displacement at *ca* 3.7 km depth and almost disappearing at 22 km; alternatively and considering the occurrence of two, sub-parallel, bands at 3.7 km depth with different resistive behaviour, one may infer the presence of two distinct SW-dipping bodies spatially organised *en échelon*. The SE sector of this southern area

displays, on the contrary, moderate- to low-resistivity ($<500 \Omega \text{ m}$), being worth to note the presence of a W–E to WNW–ESE conductor (C1) at 12 km depth ($<10 \Omega \text{ m}$). This conductor is incipiently developed at 8.4 km depth (roughly corresponding to a $50 \Omega \text{ m}$ band) but it can be clearly delimited from 12 km onwards. In the first 3 slices, a narrow resistive ($1000\text{--}2000 \Omega \text{ m}$) zone (R4) is seen to develop vertically above C1 and immediately southwards of the WNW–ESE sub-vertical corridor. At 8.4 km depth R4 collates R1, being replaced in the final slices by a moderate resistivity zone ($100\text{--}200 \Omega \text{ m}$), bordering the northern limit of C1. This strongly suggests the presence of an independent, N–NNE dipping, deep resistive body.

5. Sensitivity analysis

Due to the relatively large spacing between adjacent profiles and the loss of resolution with depth inherit to electromagnetic methods there are limits to what the MT data can resolve. This section is devoted to the analysis of the sensitivity of the MT responses to some features of the 3-D model. The importance of the high resistivity bodies

(2000 to $5000 \Omega \text{ m}$) in the north-western part of the model was investigated by computing the response for a model in which those bodies were replaced by bodies with resistivity of $500 \Omega \text{ m}$. Fig. 4A shows the comparison between the responses of our preferred model (squares and circles symbols) and this model (stars and triangles symbols) at site 11 of profile S. Making the north-western part uniformly resistive cause a larger misfit in the YX apparent resistivity and phase data in the 1 to 30 s period range. These calculations illustrate the necessity of those NW–SE resistive structures.

The influence of the conductive body labelled C2 was investigated comparing the response of a model in which the resistivity of this body was slightly changed to $50 \Omega \text{ m}$, with the response of our preferred model. The results are shown in Fig. 4B for site 4 of the profile P. Increasing the resistivity of the body C2, the YX model responses at periods longer than 10 s deviate from the observed data. Clearly, this structure must have resistivity lesser than $50 \Omega \text{ m}$.

Next, the geoelectric behaviour of the Messejana fault was addressed making the fault zone more conductive.

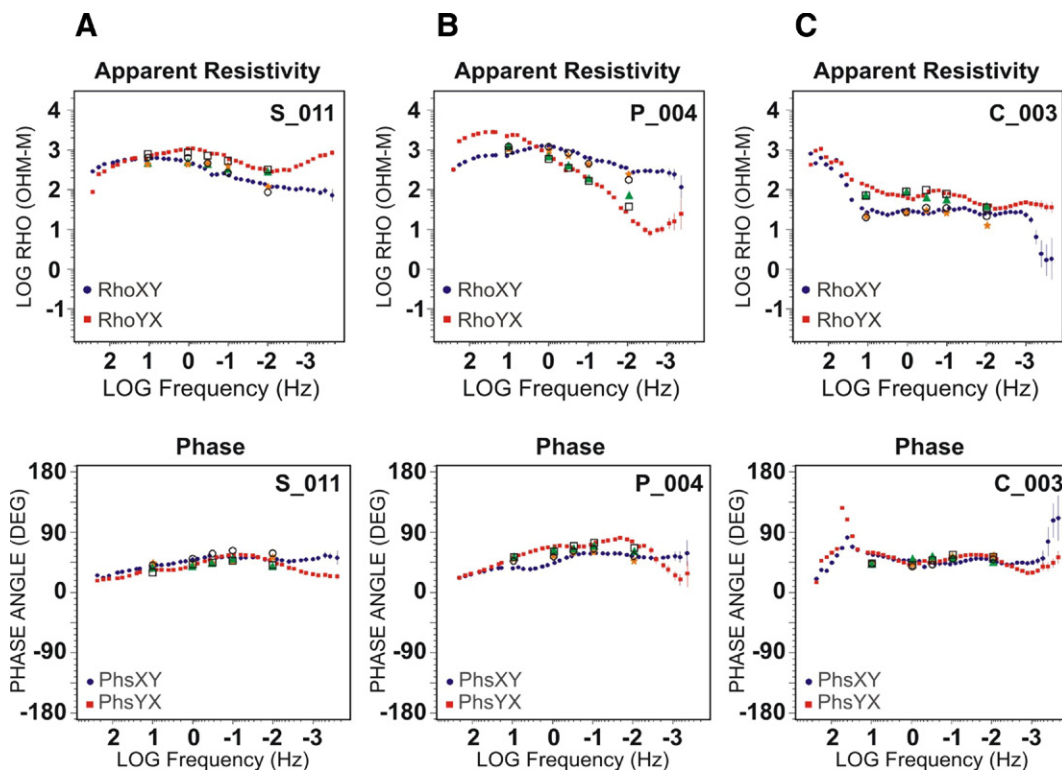


Fig. 4. Apparent resistivities and phases at three sites used in the sensitivity tests. The solid symbols correspond to the measured data. The squares and the circles correspond to the responses of the model shown in Fig. 4. The stars and triangles correspond to the responses of the modified model. A—Correspond to the response of the model when the north-western resistive bodies are replaced by uniform resistivity of $500 \Omega \text{ m}$. B—Correspond to the responses of the model where the body C2 has $50 \Omega \text{ m}$. C—Correspond to the responses of the model where the Messejana fault is represented by a $10 \Omega \text{ m}$ structure.

This was made filling the fault zone with a 10 Ω m resistivity (5 km width and 20 km thick) body. The response of this model for site 3 in profile C is shown in Fig. 4C. A small increasing of the misfit can be observed in the 1 to 10 s period range, for the YX curves and for longer periods for the XY apparent resistivity curve. Although differences between this model and our favoured model are not significant, the results of the test indicate that the Messejana fault is not a conductive structure (which is compatible with the presence of dolerite infillings), but it separates two different geoelectric domains (the more conductive one positioned to the east).

6. Discussion

The first slice in Fig. 3 offers the possibility to roughly correlate the electromagnetic imaging with the outcropping geological features. Using this correlation and considering the lithological diversity of each geotectonic unit reported in Section 2, a plausible interpretation and discussion of the electrical resistivity patterns can be performed, thus bringing some light to the nature and structure of the crust along the OMZ–SPZ boundary.

The NE–SW and WNW–ESE sub-vertical corridors represent an outstanding feature of the 3-D electromagnetic imaging, clearly separating crustal domains with distinct resistivity values. These corridors correspond indeed to two very important tectonic structures, known as the Messejana strike–slip fault zone and the Ferreira–Ficalho thrust zone, respectively. The results obtained prove that the Messejana fault zone is a very deep structure, as inferred in previous geological studies. They are also compatible with the geological deduction for the Ferreira–Ficalho thrust fault zone, strongly suggesting that the root of the WNW–ESE corridor represents the tracing of the early tectonic contact between BAOC and PLAT.

The lithological and structural features observed in OMZ are also reflected in the electromagnetic imaging obtained. In the first 500 m depth, the R2 domain integrates combined effects of different igneous intrusions and metamorphic sequences of variable nature and age. When properly limited, at 1.5 km depth, R2 matches with the deep section of the Reguengos de Monsaraz granodiorite pluton, the high-resistivity WNW–ESE band towards W corresponding to the NE border of the Évora Massif. This latter band is seen to develop till 8.4 km depth, probably representing the deeper crust level where anatectic granitoids can be found. Following this interpretation and considering the geological information so far compiled (Fig. 1A), the adjoining resistive domain (500–1000 Ω m) characterises the Proterozoic–Cambrian metamorphic sequences, which is consistent with the extension and

the electrical resistivity nature of R1. From this, a two-fold conclusion emerges: (1) the older metamorphic pile in the NW sector of the surveyed area goes much more deep than its counterpart in the SE sector, reaching at least a depth placed in the 12–22 km interval; and (2) an important tectonic structure, further re-taken by the Messejana strike–slip fault, should have had a major role in the crust configuration, bringing to shallow depths (8.4 to 12 km) the base of that pile. At this point it should be emphasised that the vertical component of movement revealed by the Messejana fault cannot justify alone that block rising, because the maximum magnitude of the accumulated vertical displacement along this structure is known to reach in some places just a few hundreds of meters. Moreover, if the Proterozoic–Cambrian metamorphic sequences were raised in the SE sector, then the C2 conductor (evident from 12 to 22 km depth) should represent the graphite-bearing granulitic basement of OMZ, as proposed in earlier studies (Almeida et al., 2001; Monteiro Santos et al., 2002; Almeida et al., 2005); note that a graphite fraction of 0.006–0.02% (occurring as interconnected films) is enough to explain the range of electrical resistivity range estimated on the basis of MT models (see calculations reported in Monteiro Santos et al., 2002). Consequently, the moderate resistivity value found above C2 (from 8.4 km onwards) is compatible either with C-enriched, meta-sedimentary rocks that underwent high-*T* metamorphism (Pous et al., 2004) or with the occurrence of a major *décollement* controlled by the rheological boundary formerly developed along the contact of the older metamorphic sequence with the crustal granulitic basement (Almeida et al., 2005).

In what concerns the OMZ unit, it should also be noted that the Variscan thrust zone separating the South-Central Belt from the Southern Crystalline Complexes does not become visible in the present electromagnetic imaging. This is probably due to poor resistive rock contrasts or boundary problems inherent to the construction of the 3-D model, since this important structure coincides with a moderate-resistive band in the 2-D imaging of Profile P (site 15 — for details see Almeida et al., 2001; Monteiro Santos et al., 2002).

The narrow and tectonically bounded belt of BAOC comprises rocks with high electrical resistivity to be found just between the OMZ border and PLAT. Meta-sediments of the latter terrane shows, typically, relatively high resistivity values, being electrically indistinct (non-contrasting) from the Palaeozoic sequences that make up the SPZ northern border; note that the available data cannot enable a real assessment of the crust structure beneath IPB. It seems thus very hard to distinguish all these geological units on the basis of

MT data, therefore limiting any assessment of their internal structure and spatial arrangement. However, a careful examination of the relative position of R3, R4 and C1 in the slices depicted in Fig. 3 gives some interesting clues that have to be discussed.

Generally, the R3 domain embraces the meta-sedimentary sequences belonging to PLAT and SPZ. The NNW–SSE tectonic contact between PLAT and OMZ mapped in the NW sector of the surveyed region is not resolved by the electromagnetic imaging. Instead, close to this contact, a high-resistive WNW–ESE band develops within PLAT from 0.5 to 12 km depth. As pointed out in Section 5, this band may represent a single body tectonically displaced or two distinct SW-dipping, *en échelon* bodies. Both possibilities are, however, compatible with the presence of hidden igneous intrusions equivalent to the Gil Marquez granodiorite in the Spanish counterpart of PLAT, whose emplacement is shown to be strongly controlled by tectonic structures related to the geodynamic evolution of this terrane (an accretionary wedge). The R4 resistive domain has probably the same geological meaning, showing continuity in the first 1.5 km depth. If so, the apparent extension towards S displayed by R1 and its connection with R3 from 3.7 to 8.4 km depths can be interpreted as a result of the R1 juxtaposition with an additional resistive band. Accepting this interpretation implies to set the base of the PLAT meta-sedimentary pile at *ca.* 3.5–5 km and to consider the WNW–ESE moderate resistivity band bounding C1 to the north as the roots of BAOC (upright during Late-Variscan tectonic adjustments). In this context, the favoured interpretation for the C1 conductor consists in its correspondence with the graphite-bearing granulitic basement of SPZ.

The depth found for C1 and C2 domains agrees with the values reported by Pous et al. (2004) for similar structures in the Spanish counterpart of the region here examined, also on the basis of MT data. In Spain, however, a straight spatial correspondence between those middle-crust conductors and the IRB is shown to exist, thus justifying the assessment of the geological plausibility of the earlier interpretations for this sub-horizontal band of high reflectivity and irregular thickness in face of the results now available.

Although accounting the possibility of IRB represent a signal of a major crustal *décollement*, Simancas et al. (2003, 2004) strongly favoured the hypothesis of this huge band (extending all over the OMZ, even though locally disturbed) correspond to a large layered sill, presumably the source of Lower Carboniferous magmas. This interpretation was adopted by several authors in order to explain the spatial distribution of early-to

late-collision magmatism in OMZ, as well as some particular geochemical features that point to relatively homogeneous crustal reservoirs (Tornos and Chiaradia, 2004; Tornos and Casquet, 2005). However, as noted by Pous et al. (2004), the presence of that igneous sill should produce a resistive rather than conductive feature, unless a multiple sheet-like intrusion separated by screens of graphite-bearing metamorphic rocks is considered. In this alternative explanation, the local increase of the conductivity is ascribed to the incorporation of variable amounts of graphite-bearing metamorphic xenoliths by the sheeted intrusion, therefore remaining open the proposition of a multiphase magma emplacement in a (very) special rheological crust level. The development of a wholesale, middle-crust igneous sill in such circumstances poses, even so, a major question that cannot be easily circumvented: What would be the geodynamic background suitable for a long-lived and widespread magma feeding (at least for *ca.* 15 Ma, if the U–Pb isotopic ages available for the less differentiated, outcropping igneous rocks are used)?

Considering the common thermal models for lithosphere (Turcotte and Schubert, 1982; England and Thompson, 1984; Davies, 1999; Poirier, 2000) and the geological framework developed during the OMZ–SPZ oblique collision, the middle-crust emplacement of that huge igneous sill implies a particular rheological framework, involving a significant crustal strength reduction that must be sustained for a relatively large time span. This can be achieved through continuous heat flow maintenance (or enhance) into the base of the crust, possibly coupled with an important mechanical discontinuity (alike to a regional *décollement* on top of the granulitic basement). The required high thermal regime in the crust should, therefore, involve a dominant heat source that can be obtained by substantial removal of the lithospheric mantle, or via crustal thickening without significant changes in mantle thickness. Delamination of the mechanical-lithosphere mantle is often invoked to explain the former process. However, evidence for an extensive mantle delamination during Variscan Orogeny seems unlikely, and even its partial elimination is extremely controversial in face of the LP–HT metamorphism and magmatism timing, besides the spatial distribution of different igneous rocks (Turpin et al., 1998; Menzies and Bodinier, 1993; Henk et al., 2000; Wittenberg et al., 2000). The second possibility should include necessarily the gradual removal of the thermal boundary layer (TBL) as collision proceeds (Houseman et al., 1981) in order to explain the long-lived and pervasive magma feeding demanded for the sill development alongside with the thermo-tectonic LP–HT Variscan metamorphism. As a result, the hot asthenospheric

mantle replacing the detached TBL heats the mechanical-lithosphere base, thereby producing magmas that will ascend and intrude at or near the Moho, advecting heat into the crust. Without magma underplating, temperatures in the crust would still rise conductively and may cause the crustal melting needed to feed the large sill, as the heat flow at the base of the lithosphere is increased. Additional constraints are, nevertheless, necessary because the formation of a (multiphase) sheet-like intrusion preserving (variably assimilated) screens of metamorphic (graphite-bearing) rocks claims for a particular contrast in viscosity and density values between the rising magma and the middle-crust rocks; and the accomplishment of these special conditions could be fortuitous.

Although strongly appealing, the TLB removal can hardly play a decisive role in the thermal regime adjustment of the OMZ crust during the oblique continental collision in Carboniferous times, even considering just the distribution of the geochemically similar, primitive igneous rocks. In fact, according to the available multi-disciplinary data, the OMZ–SPZ plate boundary should have evolved through the formation of a kinematically coupled system including a pro-wedge domain (IPB), an axial zone (PLAT) and a retro-wedge domain (the Southern Crystalline Complexes). This evolution was

favoured by a low angle subduction zone, determining the development of early-collision magmatism (*ca* 355–345 Ma), whose onset was primarily triggered by the break-off of the subducted plate (Jesus et al., 2007). Simultaneously, the stacking of fertile upper-crustal lithologies over a period of *ca.* 20 Ma (from *ca.* 360 Ma onwards) would have provide the (radiogenic) heat needed to sustain the LP–HT metamorphism and the initial steps of the late-collision magmatism, involving mixing of mantle-derived and crust-derived melts. This was followed by an important (moderate to) rapid crustal uplift episode dated of *ca.* 340 ± 5 Ma (Jesus et al., 2007) that caused a new thermal readjustment in the crust, the heat flow anomalies thus created allowing the production of late- to post-collision melts (dated from *ca* 330 to 300 Ma) and their emplacement at progressively shallower depths. In such a geodynamic scenario, the factors that ultimately may support the formation of the igneous sill presumably corresponding to the IRB only very hardly can be attained. Therefore, we are forced to conclude that the IRB should, indeed, represent a very important middle-crust *décollement*, largely developed immediately above or coinciding with the top of the OMZ granulitic basement, as schematically represented in Fig. 5.

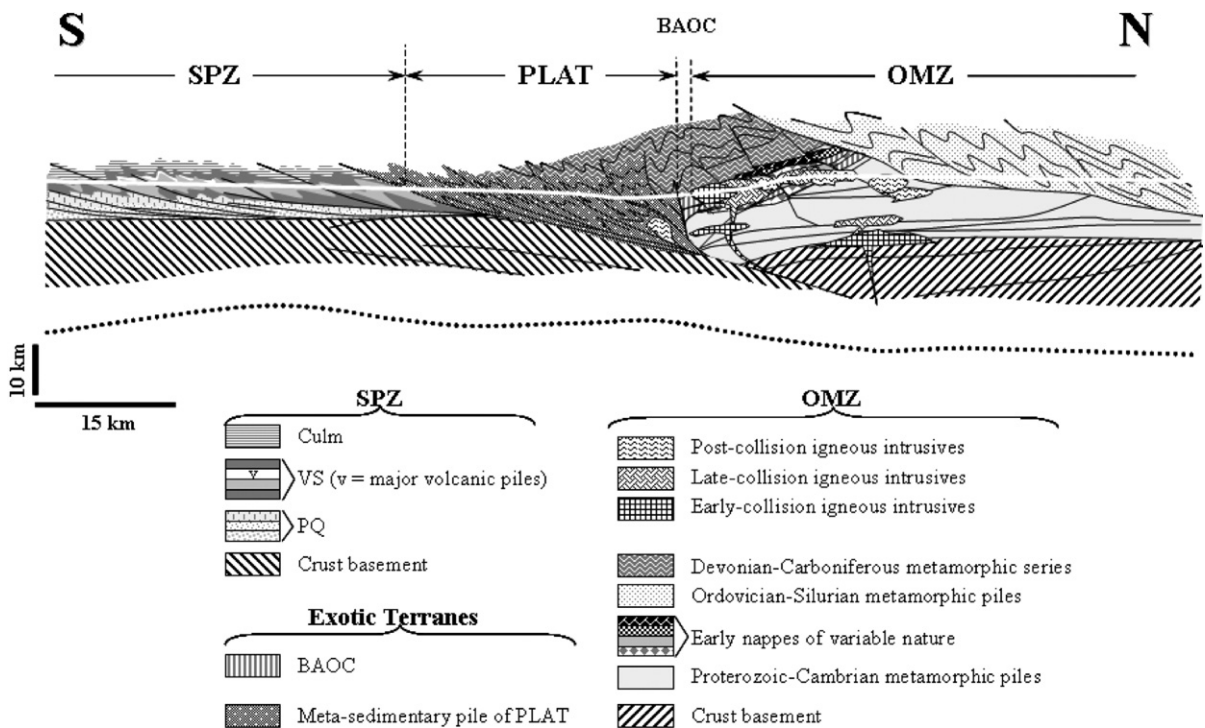


Fig. 5. Very simplified and interpretative section across the SPZ–OMZ boundary, laterally projecting the major geological formations and not considering the displacements caused by late shear zones and strike–slip fault zones. The transversal white line indicates roughly the present-day surface.

7. Conclusions

The 3-D electromagnetic imaging obtained for the OMZ–SPZ plate-tectonic boundary shows different conductive and resistive domains that display morphological variations in depth and are intersected by two major sub-vertical corridors, which coincide with the Messejana strike–slip fault zone and the Ferreira–Ficalho thrust fault zone. The former (Late-Variscan) structure, striking approximately NE–SW, divides the surveyed area into an NW and SE sector with distinct resistive behaviour at depth; the latter structure, with a general WNW–ESE direction, separates BAOC from PLAT and the correspondent resistivity contrast is particularly evident in the SE sector.

The distribution of the shallow resistive domains is consistent with the lithological and structural features observed and mapped, integrating the expected electrical behaviour produced both by igneous intrusions and metamorphic sequences of variable nature and age. The extension in depth of these resistive domains and their spatial arrangement suggest that: (1) the Precambrian–Cambrian metamorphic pile in the NW sector goes deeper (placed between 12 to 22 km depth) than its counterpart in the SE sector (located within the 8.4–12 km depth interval), thus indicating a significant vertical displacement along an early tectonic structure, subsequently re-taken by the Messejana fault-zone in Late-Variscan times; (2) hidden, syn- to late-collision igneous bodies intrude the meta-sedimentary sequences of PLAT whose base seems to lie within the 3.5–5 km depth interval; and (3) the roots of BAOC are inferred from 12 km depth onwards, forming a moderate resistive zone located between two middle-crust conductive layers extended to the north (in OMZ) and to the south (in SPZ).

The middle-crust conductive layers evidenced by MT data overlap the IRB deduced on the basis of seismic reflection data (Pous et al., 2004). Thus, the 2 s thick reflective body is also conductive, favouring the possibility of that major crustal feature correspond to an important middle-crust *décollement*, developed immediately above or coinciding with the top of a graphite-bearing granulitic basement (either in OMZ or in SPZ). This interpretation is consistent with the geodynamic evolution of the OMZ–SPZ plate boundary in Palaeozoic times and, particularly, with the geological record of the correlative thermal regime.

Comparatively to the 2-D inverted models, the 3-D model presented in this paper cannot resolve the superficial small scale geological structures. Nevertheless it has the advantage of giving a lateral definition of the main geological structures on the survey area.

Acknowledgements

The authors acknowledge the funding obtained through the Acções Integradas Luso-Espanholas and the MEC project BTE2003-03046. They appreciate also the comments and suggestions of Dr Mark Everett and of an anonymous reviewer.

References

- Abad, I., Mata, M.P., Nieto, F., Velilla, N., 2001. The phyllosilicates in diagenetic-metamorphic rocks of the South Portuguese Zone, Southwestern Portugal. *Can. Mineral.* 39, 1571–1589.
- Abalos, B., Díaz Cusí, J., 1995. Correlation between seismic anisotropy and major geological structures in SW Iberia: a case study on continental lithosphere deformation. *Tectonics* 14, 1021–1040.
- Almeida, E.P., Pous, J., Monteiro Santos, F.A., Fonseca, P., Marcuello, P., Queralt, P., Nolasco, R., Mendes Victor, L.A., 2001. Electromagnetic imaging of a transpressional tectonics in SW Iberia. *Geophys. Res. Lett.* 28, 439–442.
- Almeida, E.P., Monteiro Santos, F., Mateus, A., Heis, W., Pous, J., 2005. Magnetotelluric measurements in SW Iberia: new data for the Variscan crustal structures. *Geophys. Res. Lett.* 32, L08312.
- Andrade A.S., 1983. Contribution à l'analyse de la suture Hercynienne de Beja (Portugal), perspectives metallogéniques. Ph.D. thesis, INLP, Univ. Nancy, Nancy, France.
- Apalategui, O., Eguiluz, L., Quesada, C., 1990. Structure. In: Dallmeyer, R.D., Martinez-Garcia, E. (Eds.), *Pre-Mesozoic Geology of Iberia*. Springer-Verlag, Berlin, Germany, pp. 280–291.
- Araújo A., 1995. Estrutura de uma getransversal entre Brinches e Mourão (Zona de Ossa-Morena). Implicações na evolução geodinâmica da margem sudoeste do Terreno Atóctone Ibérico. PhD Thesis, Univ. Évora, Évora, Portugal.
- Araújo, A., Ribeiro, A., 1995. Tangential transpressive strain regime in the Évora-Aracena Domain (Ossa Morena Zone). *Bol. Geol. Min.* 106, 111–117.
- Araújo, A., Fonseca, P., Munhá, J., Moita, P., Pedro, J., Ribeiro, A., 2005. The Moura Phyllonitic Complex: an accretionary complex related with obduction in the Southern Iberia Variscan Suture. *Geodin. Acta* 18/5, 375–388.
- Arthaud, F., Matte, Ph., 1975. Les décrochements Tardi-Hercyniens du Sudoest de l'Europe. Géométrie et essai de reconstitution de la déformation. *Tectonophysics* 25, 139–171.
- Bard, J.P., Capdevilla, R., Matte, Ph., Ribeiro, A., 1973. Geotectonic model for the Iberian Variscan Orogen. *Nat., Phys. Sci.* 241, 50–52.
- Barrie, C.T., Amelin, Y., Pascual, E., 2002. U–Pb geochronology of VMS mineralization in the Pyrite Belt. *Miner. Depos.* 37, 684–703.
- Carbonell, R., Simancas, F., Juhlin, C., Pous, J., Pérez-Estaún, A., Gonzalez-Lodeiro, F., Muñoz, G., Heise, W., Ayarza, P., 2004. Geophysical evidence of a mantle derived intrusion in SW Iberia. *Geophys. Res. Lett.* 31, L11601. doi:10.1029/2004GL019684.
- Carvalho, D., Correia, H.A.C., Inverno, C.M.C., 1976. Contribuição para o conhecimento geológico do Grupo Ferreira–Ficalho. Suas relações com a Faixa Piritosa e o Grupo Pulo do Lobo. *Mem. Not. Mus. Lab. Fac. Ciências de Coimbra* 82, 145–169.
- Carvalho, D., Barriga, F.J.A.S., Munhá, J., 1999. Bimodal-siliciclastic systems — the case of the Iberian Pyrite Belt. In: Barrie, C.T., Hannington, M.D. (Eds.), *Volcanic-associated Massive Sulfide Deposits: Processes and Examples in Moderna and Ancient Settings*. Reviews in Econ. Geol., vol. 8, pp. 375–408.

- Cebriá, J.M., López-Ruiz, J., Doblas, M., Martins, L.T., Munhá, J., 2003. Geochemistry of the Early Jurassic Messejana-Placencia dyke (Portugal–Spain); implications on the origin of the Central Atlantic Magmatic Province. *J. Petrol.* 44, 547–568.
- Dallmeyer, R.D., Fonseca, P.E., Quesada, C., Ribeiro, A., 1993. $^{40}\text{Ar}/^{39}\text{Ar}$ mineral age constraints for the tectonothermal evolution of a Variscan suture in southwest Iberia. *Tectonophysics* 222, 177–194.
- Davies, G.F., 1999. *Dynamic Earth; Plates, Plumes and Mantle Convection*. Cambridge University Press, UK.
- Diáz Aspiroz, M., Castro, A., Fernández, C., López, S., Fernández Caliani, J.C., Moreno-Ventas, I., 2004. The contact between the Ossa Morena and the South Portuguese zones. Characteristics and significance of the Aracena metamorphic belt in its central sector between Aroche and Aracena (Huelva). *J. Iber. Geol.* 30, 25–51.
- England, P.C., Thompson, A.B., 1984. Pressure–temperature–time paths of regional metamorphism. Part I: heat transfer during the evolution of regions of thickened continental crust. *J. Petrol.* 25, 894–928.
- Figueiras, J., Mateus, A., Gonçalves, M.A., Waerenborgh, J.C., Fonseca, P., 2002. Geodynamic evolution of the South Variscan Iberian Suture as recorded by mineral transformations. *Geodin. Acta* 15, 45–61.
- Fonseca P., 1995. Estudo da sutura Varisca no SW Ibérico nas regiões de Serpa-Beja-Torrão e Alvito-Viana do Alentejo. PhD Thesis, Univ. Lisboa, Lisboa, Portugal.
- Fonseca, P., Ribeiro, A., 1993. The tectonics of Beja-Acebuches Ophiolite: a major suture in the Iberian Variscan Fold Belt. *Geol. Rundsch.* 3, 440–447.
- Fonseca, P., Munhá, J., Pedro, J., Rosas, F., Moita, P., Araújo, A., Leal, N., 1999. Variscan ophiolites and high-pressure metamorphism in Southern Iberian. *Ophioliti* 24, 259–268.
- Giese, U., Reitz, E., Walter, R., 1988. Contribution to the stratigraphy of the Pulo do Lobo succession in southwest Spain. *Comun. Serv. Geol. Port.* 74, 79–84.
- Gomes, E., 2000. *Metamorfismo de Rochas Carbonatadas Siliciosas da Região de Alvito (Alentejo, Sul de Portugal)*. PhD Univ. Coimbra, Coimbra, Portugal.
- Henk, A., Blanckenburg, F., Finger, F., Schaltegger, U., Zulauf, G., 2000. Syn-orogenic high-temperature metamorphism and magmatism in the Variscides: a discussion of potential heat sources. In: Frank, W., Haak, V., Oncken, O., Tanner, D. (Eds.), *Orogenic Processes: Quantification and Modelling in the Variscan Belt*. Special Publications, 179. Geological Society, London, pp. 387–399.
- Houseman, G.A., McKenzie, D.P., Molnar, P., 1981. Convective instability of a thickened boundary layer and its relevance for the thermal evolution of continental convergent belts. *J. Geophys. Res.* 86, 6115–6132.
- Jesus, A., Mateus, A., Waerenborgh, J.C., Figueiras, J., Cerqueira, L., Oliveira, V., 2003. Hypogene Ti–V maghemite accumulations in a layered gabbroic complex (Odivelas, Beja, SE Portugal). *Can. Mineral.* 41, 1105–1124.
- Jesus, A., Munhá, J., Mateus, A., Tassinari, C.C., Nutman, A.P., 2007. The Beja Layered Gabbroic Sequence (Ossa-927 Morena Zone, Southern Portugal): geochronology and geodynamic implications. *Geodin. Acta* 20 (3), 139–157.
- Julivert, M., Martínez, F.J., Ribeiro, A., 1980. The Iberian segment of the European Hercynian Foldbelt. In: Cogné, J., Slansky, M. (Eds.), *Géologie de l'Europe*. Société Géologique du Nord/BRGM, Mémoires du BRGM, vol. 108, pp. 132–158.
- Lötze, F., 1945. Zur gliederung des Variscides der Iberischen Meseta. *Geotekton. Forsch.* 6, 78–92.
- Mackie, R.L., Smith, J.T., Madden, T., 1994. Three-dimensional electromagnetic modelling using finite difference equations: the magnetotelluric example. *Radio Sci.* 29, 923–936.
- Marcoux, E., Leitell, J.A., Sobol, F., Milesi, J.P., Lascuyer, J.L., Leça, X., 1992. Signature isotopique du plomb des amas sulfures de la province de Huelva, Espagne. Conséquences Métallogéniques et Géodynamiques. *CR Acad. Sci. Paris* 314, 1469–1476.
- Marques, F.O., Mateus, A., Tassinari, C., 2002. The Late-Variscan fault network in Central-Northern Portugal. *Tectonophysics* 359, 255–270.
- Martins, L.T., 1991. *Actividade Ígnea Mesozóica em Portugal*. PhD Univ. Lisboa, Lisboa, Portugal.
- Mateus, A., Figueiras, J., Gonçalves, M.A., Fonseca, P., 1999. Evolving fluid circulation within the Variscan Beja-Acebuches Ophiolite Complex (SE, Portugal). *Ophioliti* 24, 269–282.
- Matte, Ph., 1986. Tectonics and plate tectonics for the Variscan Fold Belt in Western Europe. *Tectonophysics* 126, 329–374.
- Menzies, M.A., Bodinier, J.L., 1993. Growth of the European lithospheric mantle-dependence of upper-mantle peridotite facies and chemical heterogeneity on tectonics and age. *Phys. Earth Planet. Inter.* 79, 219–240.
- Moita, P., Munhá, J., Fonseca, P.E., Pedro, J., Tassinari, C.C.G., Araújo, A., Palácios, T., 2005a. Phase Equilibria and Geochronology of Ossa-Morena Eclogites. XIV Semana de Geoquímica/VIII Congresso de Geoquímica dos Países de Língua Portuguesa, Aveiro, Portugal, pp. 463–466.
- Moita, P., Munhá, J., Fonseca, P.E., Tassinari, C.C.G., Araújo, A., Palácios, T., 2005b. Dating Orogenic Events in Ossa-Morena Zone. XIV Semana de Geoquímica/VIII Congresso de Geoquímica dos Países de Língua Portuguesa, Aveiro, Portugal, pp. 459–461.
- Moita, P., Santos, J.F., Pereira, M.F., 2005c. Dados Geocronológicos de Rochas Intrusivas Sin-tectónicas do Maciço dos Hospitais (Montemor-o-Novo, Zona de Ossa-Morena). XIV Semana de Geoquímica/VIII Congresso de Geoquímica dos Países de Língua Portuguesa, Aveiro, Portugal, pp. 471–474.
- Monteiro Santos, F.A., Pous, J., Almeida, E.P., Queralt, A., Marcuello, A., Mati, H., Mendes Victor, L.A., 1999. Magnetotelluric survey of the electrical conductivity of the crust across the Ossa Morena Zone and South Portuguese Zone suture. *Tectonophysics* 313, 449–462.
- Monteiro Santos, F.A., Mateus, A., Almeida, E.P., Pous, J., Mendes-Victor, L.A., 2002. Are some deep crustal conductive features found in SW Iberia caused by graphite. *Earth Planet. Sci. Lett.* 201, 353–367.
- Monteiro Santos, F.A., Soares, A., Nolasco, R., Rodrigues, H., Luzio, R., Palshin, N., ISO-3D team, 2003. Lithosphere conductivity structure using CAM-1 (Lisbon-Madeira) submarine cable. *Geophys. J. Int.* 155, 1–10.
- Munhá, J., 1983a. Hercynian magmatism in the Iberian Pyrite Belt. In: Lemos de Sousa, M.J., Oliveira, J.T. (Eds.), *The Carboniferous of Portugal*. Mem. Serv. Geol. Portugal, vol. 29, pp. 39–81.
- Munhá, J., 1983b. Low-grade regional metamorphism in the Iberian Pyrite Belt. *Comun. Serv. Geol. Port.* 69, 3–35.
- Munhá, J., 1990. Metamorphic evolution of the South Portuguese/Pulo do Lobo Zone. In: Dallmeyer, R.D., Martínez-García, E. (Eds.), *Pre-Mesozoic Geology of Iberia*. Springer-Verlag, Berlin, Germany, pp. 363–368.
- Munhá, J., Oliveira, J.T., Ribeiro, A., Oliveira, V., Quesada, C., Kerrich, R., 1986. Beja-Acebuches ophiolite; characterization and geodynamic significance. *Maleo* 2 (13), 31.
- Munhá, J., Ribeiro, A., Fonseca, P., Oliveira, J.T., Castro, P., Quesada, C., 1989. Accreted terranes in Southern Iberia: Beja-Acebuches

- ophiolite and related oceanic sequences. 28th Int. Geol. Cong. (Washington, U.S.A.). Abs. with programs, vol. 2, pp. 481–482.
- Nesbitt, R.W., Pascual, E., Fenning, C.M., Toscano, M., Saez, R., Almodovar, R.G., 1999. U–Pb dating of the stockwork zircons from the eastern Iberian Pyrite Belt. *J. Geol. Soc. (Lond.)* 156, 7–10.
- Oliveira, J.T., 1983. The marine Carboniferous of south Portugal: a stratigraphic and sedimentological approach. In: Lemos de Sousa, M.J., Oliveira, J.T. (Eds.), *The Carboniferous of Portugal*. Mem. Serv. Geol. Portugal, vol. 29, pp. 3–37.
- Oliveira, J.T., 1990. Stratigraphy and syn-sedimentary tectonism in the South Portuguese Zone. In: Dallmeyer, R.D., Martinez-Garcia, E. (Eds.), *Pre-Mesozoic Geology of Iberia*. Springer-Verlag, Berlin, Germany, pp. 334–347.
- Oliveira, J.T., Cunha, T., Streeel, M., Vanguestaine, M., 1986. Dating the Horta da Torre Formation, a new lithostratigraphic unit of the Ferreira–Ficalho Group, South Portuguese Zone: geological consequences. *Comun. Serv. Geol. Port.* 72, 26–34.
- Oliveira, J.T., Oliveira, V., Piçarra, J.M., 1991. Traços gerais da evolução tectono-estratigráfica da Zona de Ossa-Morena, em Portugal. *Cuad. Lab. Xeol. Laxe* 16, 221–250.
- Oliveira, J.T., Pereira, Z., Carvalho, P., Pacheco, N., Korn, D., 2004. Stratigraphy of the tectonically imbricated lithological succession of the Neves Corvo mine área, Iberian Pyrite Belt, Portugal. *Miner. Depos.* 39, 422–436.
- Onézime, J., Charvet, J., Faure, M., Chauvet, A., Panis, D., 2002. Structural evolution of the southernmost segment of the West European Variscides. The South Portuguese Zone (SW Iberia). *J. Struct. Geol.* 24, 451–468.
- Pereira, Z., Saéz, R., Pons, J.M., Oliveira, J.T., Moreno, C., 1996. Edad devonica (Struniense) de las mineralizaciones de Aznalcollar (Faja Pirítica Iberica) en base a planinología. *Geogaceta* 20, 1609–1612.
- Pin, C., Paquette, J.-L., Fonseca, P., 1999. 350 Ma (U–Pb zircon) igneous emplacement age and Sr–Nd isotopic study of the Beja gabbroic complex (S. Portugal). In: Gamez, J.A., Eguliz, L., Palacios, T. (Eds.), *XV Reunion de Geologia del Oeste Peninsular*. Diputación de Badajoz, Badajoz, Spain, pp. 190–194.
- Poirier, J.-P., 2000. *Introduction to the Physics of the Earth's Interior*, 2nd edition. Cambridge University Press, UK.
- Pous, J., Muñoz, G., Heise, W., Melgarejo, J.C., Quesada, C., 2004. Electromagnetic imaging of Variscan crustal structures in SW Ibéria: the role of interconnected graphite. *Earth Planet. Sci. Lett.* 217, 435–450.
- Prodehl, C., Moreira, V.S., Mueller, St., Mendes, A.S., 1975. Deep-seismic sounding experiments in Central and Southern Portugal. General Assembly of the European Seismological Commission (14th - Berlin), pp. 261–266.
- Quesada, C., 1991. Geological constraints on the Paleozoic tectonic evolution of tectonostratigraphic terranes in the Iberian Massif. *Tectonophysics* 185, 225–245.
- Quesada, C., 1998. A reappraisal of the structure of the Spanish segment of the Iberian Pyrite Belt. *Miner. Depos.* 33, 31–44.
- Quesada, C., Munhá, J., 1990. Metamorphism. In: Dallmeyer, R.D., Martinez-Garcia, E. (Eds.), *Pre-Mesozoic Geology of Iberia*. Springer-Verlag, Berlin, Germany, pp. 314–320.
- Quesada, C., Fonseca, P., Munhá, J., Oliveira, J.T., Ribeiro, A., 1994. The Beja-Acebucos Ophiolite (Southern Iberian Variscan fold belt): geologic characterization and geodynamic significance. *Bol. Geol. Min.* 105, 3–44.
- Relvas J.M.R.S., 2000. *Geology and metallogenesis at the Never Corvo deposit, Portugal*. PhD Thesis, Univ. Lisboa, Lisboa, Portugal.
- Ribeiro, A., 1981. A geotransverse through the Variscan fold belt in Portugal. In: Zwart, H.J., Dornsiepen, V.F. (Eds.), *The Variscan Orogen in Europe*. Geol. Mijnbouw, vol. 60, pp. 41–44.
- Ribeiro, A., Silva, J.B., 1983. Structure of the South Portuguese Zone. In: Lemos de Sousa, M.J., Oliveira, J.T. (Eds.), *The Carboniferous of Portugal*. Mem. Serv. Geol. Portugal, vol. 29, pp. 83–89.
- Ribeiro, A., Quesada, C., Dallmeyer, R.D., 1990. Geodynamic evolution of the Iberian Massif. In: Dallmeyer, R.D., Martinez-Garcia, E. (Eds.), *Pre-Mesozoic Geology of Iberia*. Springer-Verlag, Berlin, Germany, pp. 397–410.
- Rosas, F., 2003. *Estudo tectónico do sector de Viana do Alentejo - Alvito; evolução geodinâmica e modelação analógica de estruturas em afloramentos chave (Ramo Sul ds Cadeia Varisca Ibérica — SW da Zona de Ossa-Morena)*. PhD Univ. Lisboa. 364 pp.
- San José, M.A., Herranz, P., Pieren, A.P., 2004. A review of the Ossa-Morena and its limits. Implications for the definition of the Lusitan-Marianic Zone. *J. Iber. Geol.* 30, 7–22.
- Santos, J.F., Andrade, S.A., Munhá, J., 1990. Magmatismo orogénico Varisco no limite meridional da Zona de Ossa-Morena. *Comun. Serv. Geol. Port.* 76, 91–124.
- Schermerhorn, L.J.G., 1971. An outline stratigraphy of the Iberian Pyrite Belt. *Bol. Geol. Min.* 82, 239–268.
- Simancas, J.F., Martínez Poyatos, D., Expósito, I., Azor, A., González Lodeiro, F., 2001. The structure of a major structure zone in SW Iberian Massif: the Ossa Morena/Central Iberian contact. *Tectonophysics* 332, 295–308.
- Simancas, J.F., Carbonell, R., González Lodeiro, F., Pérez Estaún, A., Juhlin, C., Ayarza, P., Kashubin, A., Azor, A., Martínez Poyatos, D., Almodóvar, G.R., Pascual, E., Sáez, R., Expósito, I., 2003. The crustal structure of the transpressional Variscan orogen of SW Iberia. The IBERSEIS deep seismic profile. *Tectonics* 22, 1062. doi:10.1029/2002TC001479.
- Simancas, J.F., Carbonell, R., González Lodeiro, F., Pérez Estaún, A., Juhlin, C., Ayarza, P., Azor, A., Poyatos Martínez, D., Almodóvar, G.R., Pascual, E., Sáez, R., Kashubin, A., Alonso, F., Alvarez Marrón, J., Bohoyo, F., Castillo, S., Donaire, T., Expósito, I., Flecha, I., Galadí, E., Galindo Zaldívar, J., González, F., González Cuadra, P., Macias, I., Martí, D., Martín, A., Martín Parra, L.M., Nieto, J.M., Palm, H., Ruano, P., Ruiz, M., Toscano, M., 2004. The seismic crustal structure of the Ossa-Morena Zone and its geological interpretation. *J. Iber. Geol.* 30, 133–142.
- Silva, J.B., Oliveira, J.T., Ribeiro, A., 1990a. Structural outline of the South Portuguese Zone. In: Dallmeyer, R.D., Martinez-Garcia, E. (Eds.), *Pre-Mesozoic Geology of Iberia*. Springer-Verlag, Berlin, Germany, pp. 348–362.
- Silva, J.B., Oliveira, J.T., Ribeiro, A., Piçarra, J.M., Araújo, A., 1990b. Thrust tectonics in the Ossa Morena Zone (South Portugal). International Conference on Paleozoic Orogens in Central Europe, Göttingen-Giesse. IGCP 233 (Abstracts).
- Siripunvaraporn, W., Egbert, G., 2000. An Efficient data-subspace inversion method for 2-D magnetotelluric data. *Geophysics* 65, 791–803.
- Soriano, C., Casas, J.M., 2002. Variscan tectonics in the Iberian Pyrite Belt, South Portuguese Zone. *Int. J. Earth Sci.* 91, 882–896.
- Strauss, G.K., Roger, G., Lécollle, M., Lopera, E., 1981. Geochemical and geological study on the volcano–sedimentary sulphide orebody of La Zarza, Huelva Province, Spain. *Econ. Geol.* 76, 1975–2000.
- Tomos, F., Casquet, C., 2005. A new scenario for the related IOCG and Ni–(Cu) mineralization: the relationship with giant mid-crustal mafic sills, Variscan Iberian Massif. *Terra Nova* 17, 236–241.
- Tomos, F., Chiaradia, M., 2004. Plumbotectonic evolution of the Ossa Morena Zone, Iberian Peninsula: tracing the influence of mantle–crust interaction in ore-forming processes. *Econ. Geol.* 99, 965–985.

- Turcotte, D.L., Schubert, G., 1982. *Geodynamics. Application of Continuum Physics to Geological Problems*. John Wiley & Sons, New York, USA.
- Turpin, L., Velde, D., Pinte, G., 1998. Geochemical comparison between minettes and kersantites from the Western European Hercynian orogen: trace element and Pb–Sr–Nd isotope constraints on their origin. *Earth Planet. Sci. Lett.* 87, 73–86.
- Van den Boorgard, M.V., 1963. Conodonts of the upper Devonian and lower Carboniferous age from Southern Portugal. *Geol. Mijnb.* 42, 248–259.
- Vozoff, K., 1991. The magnetotelluric method. In: Nabighian, M.N. (Ed.), *Electromagnetic Methods in Applied Geophysics II: Soc. Exp. Geophys.*, pp. 641–711.
- Wittenberg, A., Vellmer, C., Kern, H., Mengel, K., 2000. The Variscan lower continental crust: evidence for crustal delamination from geochemical and petrophysical investigations. In: Frank, W., Haak, V., Oncken, O., Tanner, D. (Eds.), *Orogenic Processes: Quantification and Modelling in the Variscan Belt. Special Publications*, vol. 179. Geological Society, London, pp. 401–414.